



E-ISSN: 2278-4136
P-ISSN: 2349-8234
www.phytojournal.com
JPP 2020; 9(3): 55-64
Received: 20-03-2020
Accepted: 25-04-2020

Abhishek Kumar Verma
Department of Biochemistry,
Mewar University, Gangrar,
Chittorgarh, Rajasthan, India

Santosh K Maurya
Department of Biochemistry and
Microbial Sciences, Central
University of Punjab, Bathinda,
Punjab, India

Avinash Kumar
Department of Paramedical
Sciences, Mewar University,
Gangrar, Chittorgarh,
Rajasthan, India

Dr. Mayadhar Barik
Department of Biochemistry,
Mewar University, Gangrar,
Chittorgarh, Rajasthan, India

Dr. Vipin Yadav
Department of Life Sciences,
Mewar University, Gangrar,
Chittorgarh, Rajasthan, India

Bashir Umar
Department of Biochemistry,
Mewar University, Gangrar,
Chittorgarh, Rajasthan, India

Mudassir Lawal
Department of Biochemistry,
Mewar University, Gangrar,
Chittorgarh, Rajasthan, India

Zainabm Abdullahi Usman
Department of Biochemistry,
Mewar University, Gangrar,
Chittorgarh, Rajasthan, India

Maimuna Aliyu Adam
Department of Biochemistry,
Mewar University, Gangrar,
Chittorgarh, Rajasthan, India

Bello Awal Balarabe
Department of Biochemistry,
Mewar University, Gangrar,
Chittorgarh, Rajasthan, India

Corresponding Author:
Abhishek Kumar Verma
Department of Biochemistry,
Mewar University, Gangrar,
Chittorgarh, Rajasthan, India

Inhibition of multidrug resistance property of *Candida albicans* by natural compounds of parthenium hysterophorus L. An *In-Silico* approach

Abhishek Kumar Verma, Santosh K Maurya, Avinash Kumar, Dr. Mayadhar Barik, Dr. Vipin Yadav, Bashir Umar, Mudassir Lawal, Zainab Abdullahi Usman, Maimuna Aliyu Adam and Bello Awal Balarabe

DOI: <https://doi.org/10.22271/phyto.2020.v9.i3a.11480>

Abstract

Objectives: In this study, we targeted enzymes (Erg11, Erg5, Erg3), transporters (CDR1, CDR2), and cytochrome 450 (CaALK8) involved in MDR of *Candida albicans*, which caused fungal disease. ATP-binding cassette (ABC) and some other major facilitator superfamilies (MFS) of transporters are responsible for MDR in *Candida Albicans*.

Material and methods: The compounds present in *Parthenium hysterophorus* L. were docked against the proteins involved in MDR of *Candida Albicans*. PyRx-Python prescription 0.8. was used to identify binding affinities of compounds against the proteins.

Result and Discussion: Erg11, Erg5, Erg3, CDR1, CDR2 and CaALK8 proteins docked with β -Sitosterol (-10.6, -9.6, -9.6, -9.6, -9.6, and -8.5) ζ -Sitosterol (-9.9, -9.2, -9.3, -9.4, -9.6, and -8.5). Piperine (-10.0, -8.3, -9.3, -8.4, -8.5, and -8.4) Kcal/mol respectively and found to show good hydrophobic interactions.

Conclusion: In this study, we may conclude that compounds isolated from *parthenium hysterophorus* might be effective against the fungal disease caused by *Candida Albicans*.

Keywords: *Parthenium hysterophorus*, *Candida Albicans*, MDR, *in silico*

Introduction

According to a rise in the number of patients used in patients undergoing organ transplants, anticancer chemotherapy, and Hiv patients, the incidence of widespread fungal infection has risen significantly in recent years.

Candida infections are significant, morbidity and death effects and are related to a wide variety of clinical symptoms to the surface and mucosal infections are common; and also bloodstream infections. *Candida albicans* a leading source of candidemia, but also *Candida* species (non-*albicans*) account for >50 percent of blood disease in many parts of the world [Kullberg *et al.*, 2015]. Global estimates suggest that, in population-based trials, invasive candidiasis occurs in over a quarter of a million patients each year with incidence rates of 2–14 candidates per 100,000 inhabitants [Bitar *et al.*, 2014; Cleveland *et al.*, 2012; Magil *et al.*, 2012]. Resistance to antifungal agents is less common in *C. Albicans* with long-term anti-mucosal usage and recurring disease, such as persistent mucocutaneous candidiasis or recurring oropharyngeal candidiasis, have been identified in patients with unregulated HIV infection. Resistance to > 1 class of drugs (multidrug resistance) remains rare but has been slowly reported, for example in *Candida Auris*. Genetic and molecular resistance mechanisms have been identified for many strains and understanding of these mechanisms can aid guide selection of therapies. Diagnosis remains difficult in these patients but is critical. Due to the increased susceptibility of immunocompromised patients, opportunistic *Candida albicans*, and some other organisms have gained significance in the past [Arendrup & Patterson, 2017].

Candida species and derive their importance from the severity of their infections to their ability to develop resistance to antifungals. Azoles and its widespread use contributed to the accelerated growth of the MDR syndrome, which poses a significant challenge in fungal therapy. Different pathways that lead to the production of MDR have been involved in

Candida and in other human fungal infections, some of which include overexpression or mutation in the target enzyme of lanosterol 14 α -demethylase, azoles, and activation of drug-encoding pump proteins belonging to the ATP-binding sequence (ABC) and main facilitator genes. ABC transporters, CDR1 and CDR2, play a crucial role in azole tolerance, as deduced from their elevated degree of expression found in many clinical isolates with azole resistance.

Throughout India, several plants are considered to have therapeutic qualities, and the use of different components of many therapeutic flowers for particular therapy conditions has become fashionable because of ancient instances [Parekh *et al.*, 2005] [5]. Food-based antimicrobials are a huge untapped source of medicinal products even after their considerable therapeutic potential and efficacy in the treatment of infectious disease subsequently, plant antimicrobials need to be investigated similarly [Parekh *et al.*, 2007] [11]. Mainstream medicine becomes gradually sensitive to the use of antimicrobials and other flora-derived drugs, as traditional antibiotics are obsolete, and due to the accelerated loading of plant species extinction, Medicinal plants are useful medicinal properties and appeared to be unquestionably healthy pills and were even tested for edible, antimicrobial and hypoglycemic hobbies. [Bhat *et al.*, 2009] [1]. Recently scientific interest in medicinal plants has burgeoned due to the increased success of plant-derived pills and the subject has posed about the facet effects of the modern-day remedy. In the dominant, take a look at what has been done to determine the anti-fungal value of the *Parthenium hysterophorus L.* Incomptin B and ambrosin, which are isolated from *parthenium hysteropous L.*, were found to use against the Chagas disease caused by *Trypanosoma cruzi* [Sepulveda-Robles *et al.*, 2019]. In a study, it has been shown that extracts isolated from *parthenium hysteroporus L.* useful in the inhibition of growth and colonization of *helicobacter pylori* [Espinosa-Rivero *et*

al., 2015]. In this study, we analyzed the role of parthenium compounds on MDR of candida Albicans using *in silico* tools and techniques.

Materials and Methodology

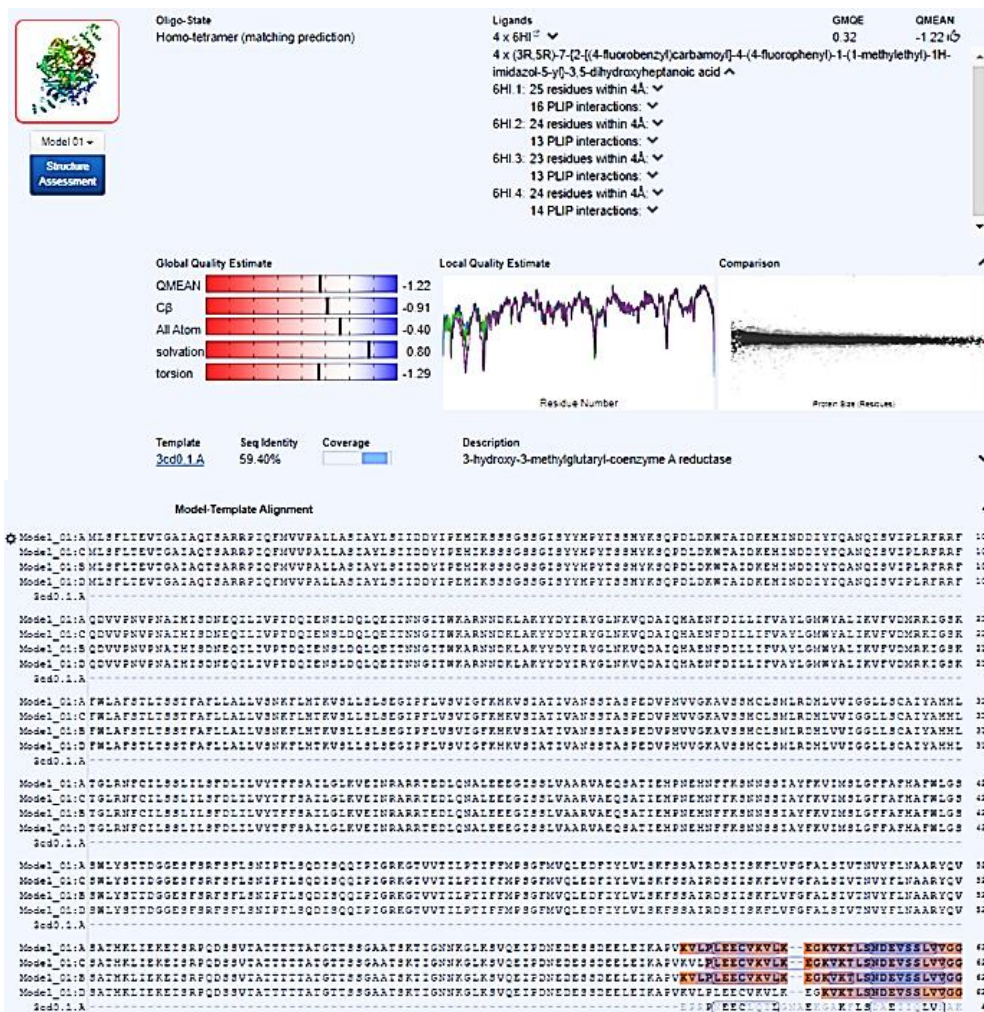
Protein Preparation

The protein structures of target proteins CDR1 (5d07), CDR2 (5do7), Erg11 (5v5z), Erg3, Erg5(5e0e), and CaALK8 (2fdu) were sourced from RCSB Protein Data Bank in .pdb format.

Retrieval of Proteins

A- Homology Modeling

Homology modeling approaches use experimental protein structure ("templates") to construct drug discovery receptor proteins. Homology modeling is probably the most effective tool for producing robust tridimensional models of protein structure. Swiss-model is a web-server of structural bioinformatics devoted to modeling homology for the analysis of 3d protein structures (Chothia C, LesKAM, 1986; Kaczanowski, Zielenkiewicz, 2010) [4, 8]. The whole protein was modeled by uploading the ERG3 protein FASTA sequence into the SWISS-MODEL workspace via automatic mode for the creation of a more reliable protein model (20). The ERG3 protein and its sequence, respectively, were selected as the target protein and query sequence. The HMG1 crystal structure was derived from a sample of proteins. The model for the ERG3 protein was developed using the HMG1 protein as a reference sui Table No. Four-four templates of query sequences were created in automatic mode at the SWISS-MODEL workplace. The prototype, 3cd0.1.c demonstrated to query sequence the highest sequence identity, which was used to create an improved ERG3 protein model. Global quality estimate, local quality estimate comparison, and ERG3 model template alignment with 3cd0.1.c, were calculated (figure 1).



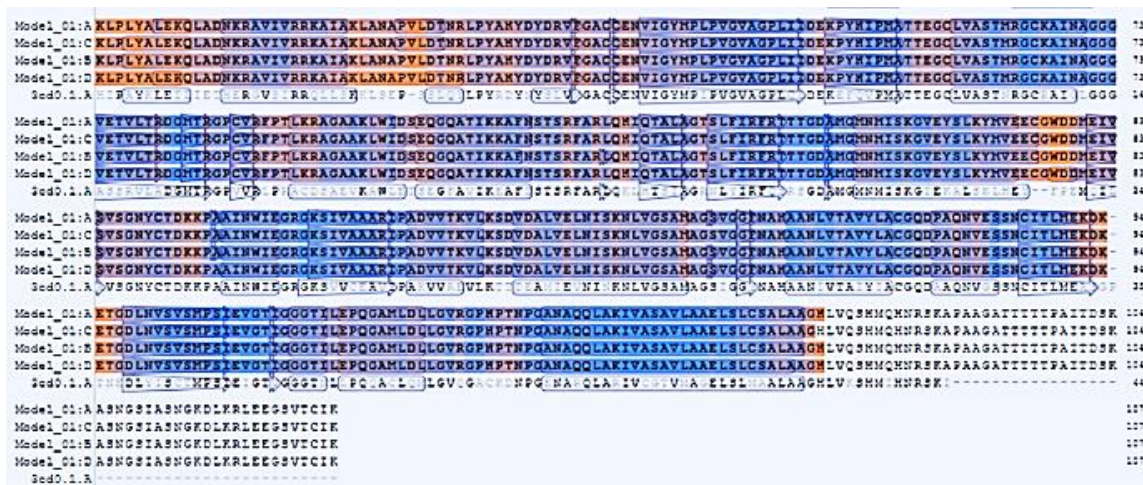


Fig 1: Global quality estimate, local quality estimate comparison and Erg3 model template alignment with 3cd0.1.c

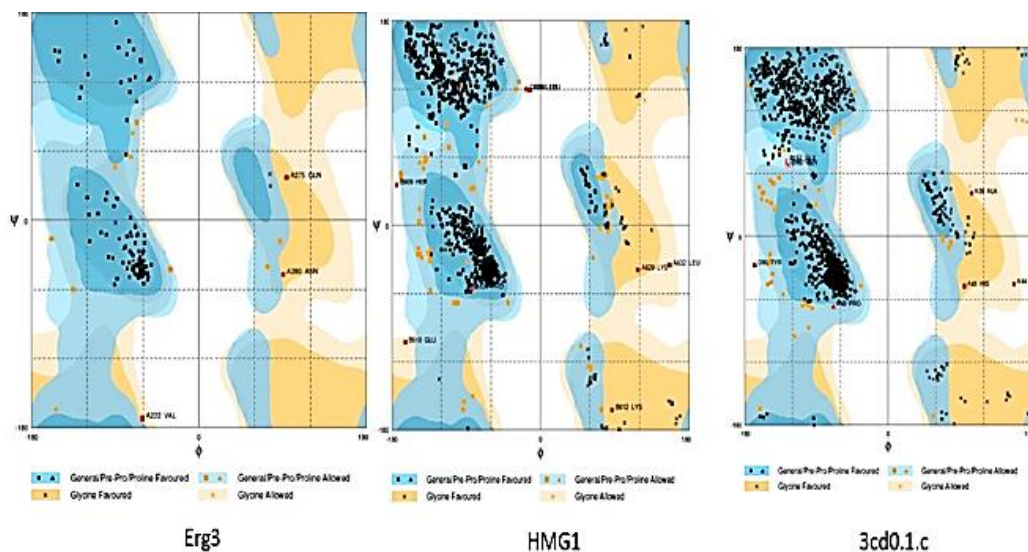
B. Modeled ERG3 protein validation

Homology simulation approaches in drug development use experimental protein structures ("templates") to construct a protein. Homology (or comparative) modeling is probably the most effective way of producing consistent tridimensional patterns of protein structure. SWISS-MODEL is a web-server of computational bioinformatics devoted to modeling homology for predicting 3D protein structures (Chothia C, LesKAM, 1986; Kaczanowski, Zielenkiewicz, 2010) [4, 8]. The structure contains a few amino acid residues that are absent. The ERG3 protein was modeled by applying the HMG1 protein FASTA sequence to the SWISS-MODEL workspace by automated mode for the SWISS-MODEL workspace by automated mode for the creation of a specific protein model (Bordoli *et al.*, 2008) [3]. The ERG3 protein and its sequence, respectively, were selected as the target protein and query sequence. The protein model was built using 3cd0.1.c, the protein as a template suitable No. (Fig. 1). Ramachandran plot validated the ERG3 protein output using Rampage (Read RJ *et al.*, 2011) [13] and SPDBV (Deep View-Swiss-Pdb Viewer) version 4.10, based on the RMSD value

obtained by superimposing the ERG3 protein model on its 3cd0.1.c, (Savarino A *et al.*, 2007) [14] model design. The ERG3 based protein plot values for Ramchandran and its 3cd0.1.c template were obtained (Table No. 1). In the Erg3 protein Ramachandran plot, 90.4 percent of the amino acid residues were found in the favored region, 7.4 percent residues in the permitted region, and 2.2 percent of the residues in the outer regions (Figure 2). For the 3cd0.1.c, the Ramachandran plot displayed 95.3 percent, 4.7 percent, and 0 percent, respectively, of the residues in the favored, permitted, and outer regions. The Ramachandran plot data for the Erg3 and 4zr0 modeled proteins suggested favorable reliability of the ERG3-modelled protein for subsequent docking studies (Table 1) (Figure 2).

Table 1: The data from Ramachandran plot of the Erg3

Percent (%) of residues per region			
Structure	Favored	Allowed	Outlier
Erg3	90.4%	7.4%	2.2%
HMG1	95%	4.5%	0.5%
3cd0.1.c	96.4%	3.1%	0.5%



Library Preparation

The various literature database searched for the occurrence of phytochemicals in *Parthenium hysterophorus L.* At the end of the literature survey, we found the presence of phytochemicals in *Parthenium hysterophorus L.* leaves, stem, and root.

The literature-based 3D or 2D structure of phytochemicals of Target proteins CDR1, CDR2, $\Delta^5,6$ -desaturase (Erg3), Lanosterol 14- α demethylase (Erg11), C-22 sterol desaturase (Erg5), alkane assimilating cytochrome P450 (CaALK8), and the modeled protein was retrieved in .sdf format from NCBI PubChem. For the conversion of 2D to 3D conformation, open Babel molecule format converter was used, Marvin Sketch software (version 15.10.0) performed the conversion from .sdf to .pdf (for docking) and mol (for molecular properties prediction) file. For the were prepared using Marvin Sketch. Ligand's energy was minimized by relating the mmff94 force field and conjugate gradients optimization algorithm using PyRx- Python prescription 0.8 for 200 steps (Dallakyan *et al.*, 2015).

ADME/T Properties

For the estimation of the ADMET properties, a statistical analysis of natural compounds was carried out. In this analysis, we evaluated ADMET properties using the ADMET predictor FAFDrugs2 that runs on Linux OS. This method is freely available and used for filtering in silico ADME/T. (Lagorce *et al.*, 2008) [5]. This technique has been widely used as a screen for compounds that are expected to be produced more for product design programs. We have tested parameters such as the number of rotatable No. bonds (> 10) and the number of rigid bonds that suggest good oral bioavailability and good intestinal absorption of the compound (P. Ertl *et al.*, 2000) [10].

Virtual screening and blind Molecular Docking

Crystal structure of target CDR1, CDR2, Erg11, Erg3, Erg5, and CaALK8 were obtained from the RCSB protein data bank along with the structure of a protein that has been modeled. The groundwork of the target enzyme with Auto Dock Tools involved in the adding of hydrogen atoms to the target enzyme, which is an essential step for the compilation of partial atomic charges. Gasteiger charges will be measured for each atom present in the target in Auto Dock 4.2.

To dock small-molecule libraries to a macromolecule virtual molecular screening is used to hit upon lead compounds with preferred biological function. In PyRx software, we perform docking of the ligands and protein. PyRx software is open version software with an intuitive user interface that runs on all major operating systems (Linux, Windows, and Mac OS) (Trott and Olsen 2009) [16]. receptor-based molecular docking was conducted using GLIDE software from PyRx-Python prescription 0.8. Each of these phytochemicals was docked into target protein therefore with positions, orientations, and conformations of the ligand in the receptor-binding site, and the docking structure keeping the lowest energy was preferred (Singh *et al.*, 2015). The ligands and proteins were loaded into ADT for docking experiments. After merging non-polar hydrogen and torsions realistic to the ligands by rotating all rotatable No. bonds Gasteiger partial charges are assigned Docking calculations approved out on the protein models. With the aid of Auto Dock tools polar hydrogen atoms and solvation parameters were added. ADT offers the option of three search algorithms to walk around the space of active binding with different efficacy. The content of configure file

was determined as position of receptor/enzymes file, ligand file, data of Grid- box's three coordinates X, Y, Z were -22.0141, 14.2175, 19.8284 respectively in case of Erg11, -2.7205, -35-1188, -58.4468 for CDR1 and CDR2, 82.6642, 44.3460, 126.4895 in Erg3, -15.3468, 18.0274, -11.3394 in Erg5, 50.04650, 55.9125, 78.3741 in CaALK8, the size of Grid Box which was set up in 25 X 25 X 25 points. The grid box includes the whole binding site of the proteins line and provides sufficient space for the ligands translational and rotational walk. After that, PyRx-Python prescription 0.8 is used for visualization of the interaction pattern in the protein-ligand complex (Humphrey *et al.*, 1996) [6].

Protein-Ligand Interaction and LigPlot

The protein-ligand complexes in the .pdb format are displayed, edited, and run via the software Lig-Plot+ (version v.1.4.5) for the generation of Lig-Plot Schematic Diagrams. The protein-ligand interactions along with the hydrophobic interactions and hydrogen bonding with the complex binding residues are given for the lead phytochemicals. The Lig-Plot shows the amino acid of the target protein which is involved in the interaction with the ligand. The interaction profile of lead phytochemicals and the interface among heterodimers of a protein can be determined. The amino acid involved in hydrophobic interaction and hydrogen bonding with the ligands can also be easily determined.

Protein-ligand binding surface-structure determination

The modified ligands binding with active sites of the targeted protein is determined and visualized by surface structure determination of ligand and protein binding. It is a molecular modeling technique whereby the interaction between the protein-ligands is determined by the position and orientation of the ligand when bound to the protein. The surface structure of the protein and ligand is determined through PyMOL Molecular Graphics System Software (version 1.1). The modified pdbqt files of proteins and ligands are prepared and displayed in PyMOL which gives a commendable visualization of the protein-ligand interaction. The best docking score of protein is chosen with the ligands having the best binding affinity and the surface structure was prepared.

Results and Discussion

Ligand-Protein Binding Analysis

The present docking study explored the interactions of selected standard ligands, β -Sitosterol, γ -Sitosterol, and Piperine against the proteins such as Erg11 (-9.6, -10.6, -9.9, and -10.0), CDR1 (-6.9, -9.6, -9.4, and -8.4), CDR2 (-5.6, -9.5, -9.6, and 8.5), ERG5 (-7.6, -9.6, -9.2, and -8.3), ERG3 (-8.7, -9.6, -9.3, and -9.3), and CaALK8 (-8.0, -8.5, -8.6, and -8.4) show that our selected ligands are found to bind with higher binding affinity than standard drugs (Fig. 3-8).

We have taken some of the proteins, which take part in the process of MDR, in which Erg11, Erg5, Erg3 are enzymes, CDR1, CDR2 are transporters, and CaALK8 is cytochrome 450. Our docking result shows that good docking between our selected compounds and these proteins.

Protein-ligand interaction

There is some interaction like hydrophobic interactions and hydrogen bonding between amino acids of proteins and selected compounds. Mostly it has been found that hydrophobic interaction plays a very important role in strongly binding atoms of ligands and amino acids of proteins. Erg11 protein molecule create hydrophobic interactions with

the help of Pro 238, Leu96, Phe384, Arg98, Ala69, Thr507, Val242, Met100, Phe338. CDR1 protein has found to create interaction through Tyr564, Leu637, Ala633, Phe630, Ile626, Leu637 amino acid. CRD2 protein interacts with ligands with the help of Phe567, Phe565, Leu637, Ala633, and Leu634. ERG3 binds with ligands with Phe263, Val264, Thr262, Phe231 amino acids. In a case in ERG5, Phe206, Glu301, Phe297, Glu218 was found to form hydrophobic interactions

with elected compounds. CaALK8 binds with compounds with the help of Phe211, Gln210, Thr214, Ala237, Gln236, Pro233, Thr214 amino acids (fig 9-14).

Selected proteins are found to show good hydrophobic interaction and hydrogen bonding with the amounts of selected compounds. These hydrophobic interactions formed between the proteins and compounds show the strength of the interaction.

Table 2: Molecular docking of proteins and compounds

Protein targets	Binding Affinity (Kcal/mol)			
	Standard drugs	(β -Sitosterol) CID-222284	(ζ -Sitosterol) CID-457801	(Piperine) CID-638024
ERG11	-9.6 (Azoles)	-10.6	-9.9	-10.0
CDR1	-6.9 (Flucanazole)	-9.6	-9.4	-8.4
CDR2	-5.6 (Ceruleinin)	-9.5	-9.6	-8.5
ERG5	-7.6 (Flucanazole)	-9.6	-9.2	-8.3
Erg3	-8.7 (Azoles)	-9.6	-9.3	-9.3
CaALK8	-8.0 (Cycloheximide)	-8.5	-8.6	-8.4

ADME/T prediction of selected compound

Through using FAFDrugs2 and data outlined in Table No. we had examined various physical descriptors and pharmaceutically important properties for ADME/T prediction. All of the substances showed important values for the various criteria tested and displayed strong drug-like properties based on the five law of Lipinski. The data obtained were within the range of values for all-natural compounds. The importance of polar surface area (PSA) suggested good oral bioavailability for natural compounds (β -Sitosterol, ζ -Sitosterol, and Piperine). The parameters, such as

number of rotatable No bonds and number of stable bonds correlated with the product of intestinal absorption, revealed that all-natural compounds (β -Sitosterol, ζ -Sitosterol, and Piperine) are well absorbed. All the synthesized compounds were found to be nontoxic (Table No. 4).

Online we have done ADME/T prediction, which shows our selected ligands follow all Lipinsky's rule of five. In our study, we can conclude that a selected compound is good to inhibit all of the proteins involved in MDR and will be a useful aspect to prevent fungal disease caused by Candida Albicans.

Table 3: Protein-Ligands Interaction and Lig-Plot

Erg11	Standard (Azoles)	H-Bonding	Phe241(A), His405(A)
		Hydrophobic Interactions	Pro238(A), Leu95(A), Arg98(A), Phe384(A), His128(A), Ala125(A), Leu96(A), Val242(A),
	β -Sitosterol	H-Bonding	- -
		Hydrophobic interactions	Met100(A), Val242(A), Leu96(A), Leu95(A) Arg98(A), Phe241(A), Phe384(A), Tyr72(A) Thr507(A),Pro238(A), His381(A), Gly73(A), Ala69(A)
	ζ -Sitosterol	H-Bonding	-
		Hydrophobic interactions	Ala69(A), Arg98(A), Leu96(A), Met100(A), Val242(A), Leu95(A), Phe241(A), Gly73(A), His381(A), Tyr72(A), Pro238(A), Phe384(A), Thr507(A)
	Piperine	H-Bonding	-
		Hydrophobic interactions	His405(A), Phe241(A), Phe384(A), Thr507(A), Val242(A), Pro238(A), Arg98(A) Ala125(A), His128(A)
CDR1	Standard (Flucanazole)	H-Bonding	Gln442(B), Lys614(B), Tyr613(B)
		Hydrophobic Interactions	Arg522(B), Arg211(B), Asn520(B), Phe608(B), Leu443(B), Gln607(B)
	β -Sitosterol	H-Bonding	Tyr564(C)
		Hydrophobic Interactions	Ser629(A), Phe630(A),Ile626(A),Val640(C), Tyr564(A),Leu637(C), Ile636(C),Tyr570(A), Ala633(C), Ala633(A), Phe630(A), Tyr570(C), Ile626(C), Leu637(A)
	ζ -Sitosterol	H-Bonding	-
		Hydrophobic interactions	Phe461(B),Tyr567(B), Gly428(A), Tyr432(A) Asn564(B), Phe561(B), Ile395(A), Phe399(A) Met396(A), Asn568(B), Tyr571(B), Ile539(A)
	Piperine	H-Bonding	-
		Hydrophobic interactions	Leu516(C), Phe565(A), Tyr564(A), Phe630(A), Ile626(A), Leu637(C), Ala633(C) Leu637(C),Leu634(C), Phe630(C)
CDR2	Standard (Ceruleinin)	H-Bonding	His557(D),Asn564(D), Asn531(C), Tyr432(C)
		Hydrophobic Interactions	Met396(C), Thr433(C), Leu436(C), Phe561(D), Ser560(D)
	Inhibitor	H-Bonding	Gln568(A), Leu537(A),

	β -Sitosterol	Hydrophobic Interactions	Phe567(A), Thr566(A), Phe565(A), Leu637(A), Phe565(C), Tyr564(C),Ala633(A) Leu634(A), Phe630(A), Ser538(A), Gly541(A)
	ζ -Sitosterol	H-Bonding	-
		Hydrophobic Interactions	Tyr571(D), Ile539(C), Asn568(D), Phe461(D) Tyr432(C), Phe561(D), Asn564(D), Ala565(D), Ile395(C), Phe399(C), Met396(C) Tyr567(D), Gly428(C), Gln425(C)
Piperine	H-Bonding	-	
	Hydrophobic Interactions	Leu516(A), Phe630(A), Phe565(C), Tyr564(C), Phe630(C), Ile626(C), Leu637(A) Ala633(A), Leu634(A), Phe567(A)	
Erg3	Standard (Azoles)	H-Bonding	-
		Hydrophobic Interactions	Arg750(B), Val895(A), Ser891(A),Met938(C) Leu937(C), Glu939(C), Lys940(C), Val886(C), Glu887(A), Ile890(A)
	β -Sitosterol	H-Bonding	Arg750(D)
		Hydrophobic Interactions	Glu887(C), Val886(C), Ser891(A), Ile890(A), Ile890(C), Glu939(C), Met938(C), Arg750(B) Glu887(A), Lys940(C), Val886(A), Lys940(A)
	ζ -Sitosterol	H-Bonding	Phe266(A), Ser268(A)
		Hydrophobic Interactions	Ala230(A), Val269(A), Phe263(A), Thr262(A), Phe261(A), Ser240(A), Phe231(A), Val264(A)
	Piperine	H-Bonding	Tyr246(A), Ser240(A)
		Hydrophobic Interactions	Phe192(A), Phe189(A), Thr193(A), Phe263(A), Gly196(A), Val264(A), Phe231(A), Pro233(A), Gly236(A), Thr262(A), Tyr243(A)
Erg5	Standard (Flucanazole)	H-Bonding	Lys479(A)
		Hydrophobic Interactions	Glu301(A), Gly478(A), Thr305(A), Leu362(A), Ala298(A),Ile363(A),Phe206(A)
	β -Sitosterol	H-Bonding	-
		Hydrophobic Interactions	Leu219(A), Phe206(A),Glu301(A), Phe297(A), Val103(A), Gln(215), Glu218(A), Leu70(A), Leu43(A)
	ζ -Sitosterol	H-Bonding	-
		Hydrophobic Interactions	Pro368(A), Ile209(A), Val367(A),Phe115(A) Ile363(A), Val114(A), Ala298(A),n Phe297(A), Thr302(A), Ile101(A), Glu218(A)
	Piperine	H-Bonding	Arg308(A), Gln172(A),
		Hydrophobic Interactions	Thr168(A), Val480(A), Ser207(A), Gly478(A), Ser210(A), Ile209(A), Phe206(A) Glu301(A), Tyr(203)
CaALK8	Standard (Cycloheximide)	H-Bonding	-
		Hydrophobic Interactions	Val117(A),Leu298(A), Cys439(A), Asn438(A),Ser433(A),Ile366(A),Leu395(A), Phe432(A), Leu370(A), Gly301(A), Phe440(A), Phe441(A),
	β -Sitosterol	H-Bonding	Gln236(B)
		Hydrophobic Interactions	Phe211(B), Gln210(B), His477(B), Glu52(B) Thr214(A), Ser215(A), Phe211(A), Ala237(A), Gln236(A), Pro233(A), Gln210(A), Gly207(A), Thr214(B)
	ζ -Sitosterol	H-Bonding	Gly207(B), Gln236(B)
		Hydrophobic Interactions	Phe211(B), Gly52(A), Gln210(B), Thr214(B), Glu52(B), Gln236(A), Gln210(A), Ala237(A), Phe211(A), Pro233(A), Thr214(A), Thr216(A)
	Piperine	H-Bonding	Asn297(B)
		Hydrophobic Interactions	Phe111(B), Ile300(B), Phe209(B), Phe107(B) Ile366(B), Cys439(A), Phe432(B), Ser433(B), Ser369(B), Leu370(B), Phe118(B), Leu296(B)

Table 4: Prediction of ADMET Properties of compounds.

Compounds (Pubchem Id)	MW	logP	AlogP	HBA	HBD	TPSA	AMR	nRB	nAtom	nAcidic	RC	nRigidB	nAromatic Ring	nHB	Toxicity
457801	414.39	11.59	1.3	1	1	20.23	123.88	6	80	0	4	27	0	2	Non-toxic
222284	414.39	11.59	123.88	1	1	20.23	123.88	6	80	0	4	27	0	2	Non-toxic
638024	285.14	2.51	-0.63	4	0	38.77	38.03	4	40	0	3	19	1	4	Non-toxic

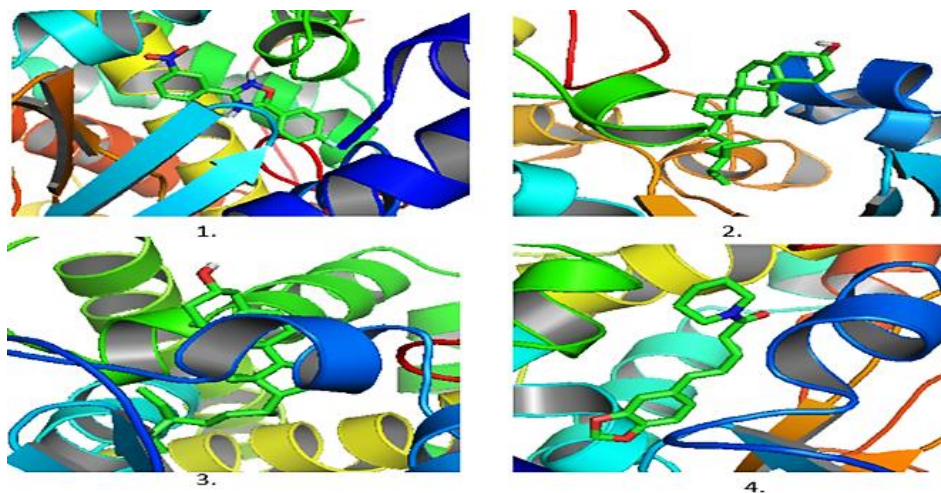


Fig 3: Ribbon representation of of protein-ligand complex (1) ERG11-Cyclohexamide (Standard) (2) ERG11- β -Sitosterol (3) ERG11- ζ -Sitosterol (4) ERG11-Piperine.

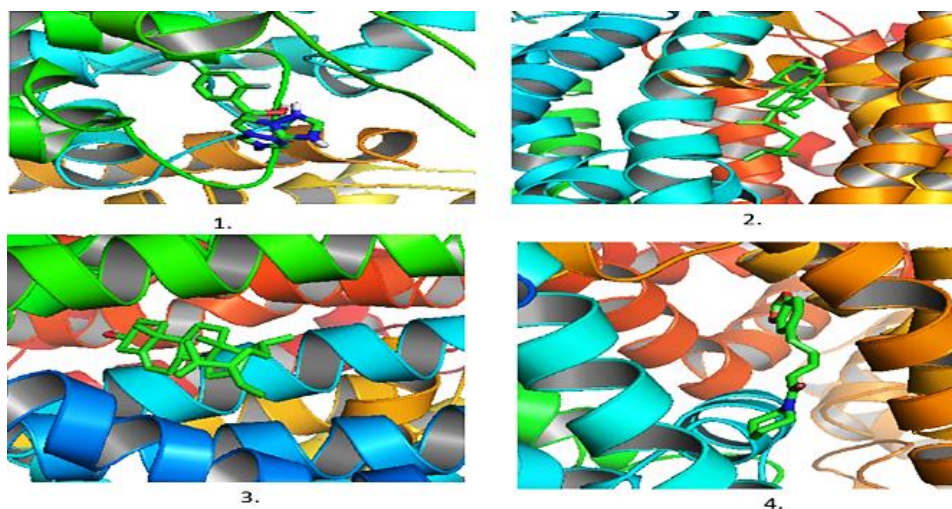


Fig 4: Ribbon representation of of protein-ligand complex (1) CDR1-Cyclohexamide (Standard) (2) CDR1- β -Sitosterol (3) CDR1- ζ -Sitosterol (4) CDR1-Piperine.

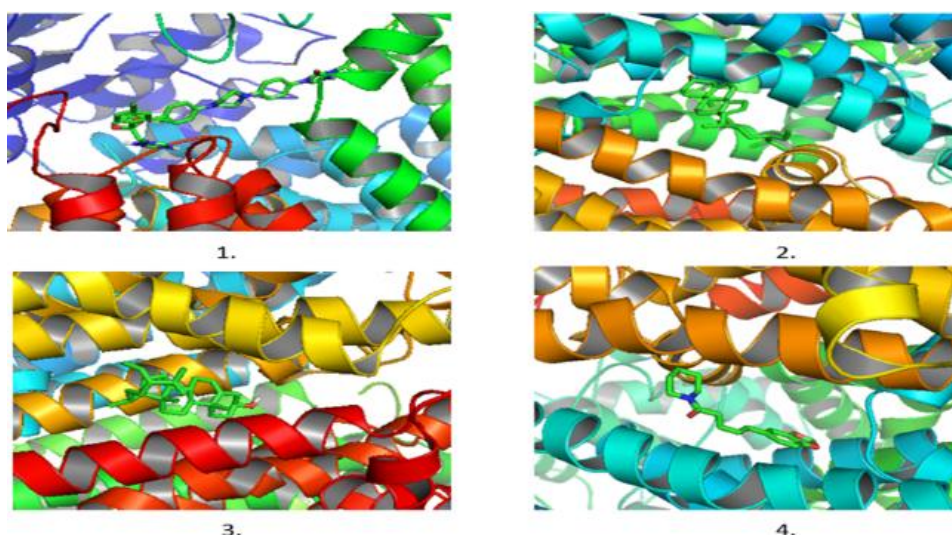


Fig 5: Ribbon representation of of protein-ligand complex (1) CDR2-Cyclohexamide (Standard) (2) CDR2- β -Sitosterol (3) CDR2- ζ -Sitosterol (4) CDR2-Piperine.

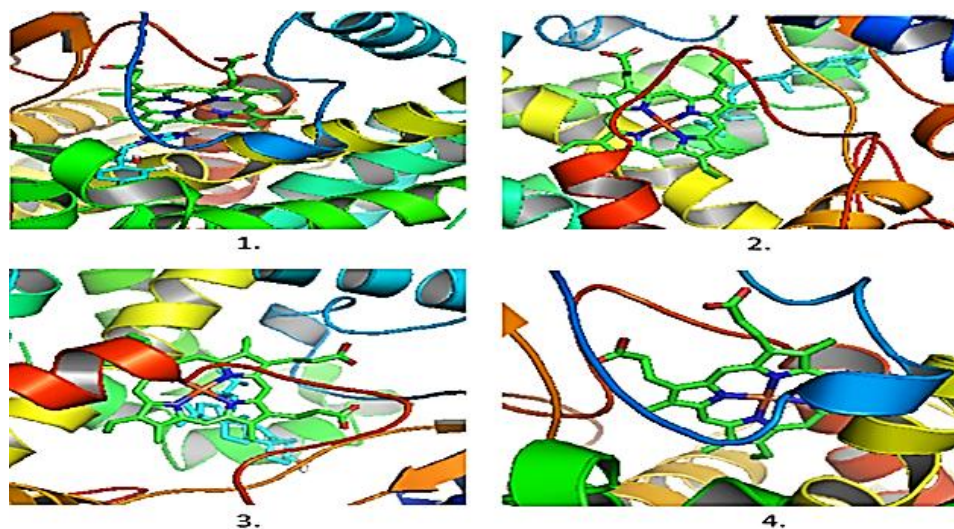


Fig 6: Ribbon representation of of protein-ligand complex (1) ERG5-Cyclohexamide (Standard) (2) ERG5- β -Sitosterol (3) ERG5- ζ -Sitosterol (4) ERG5-Piperine.

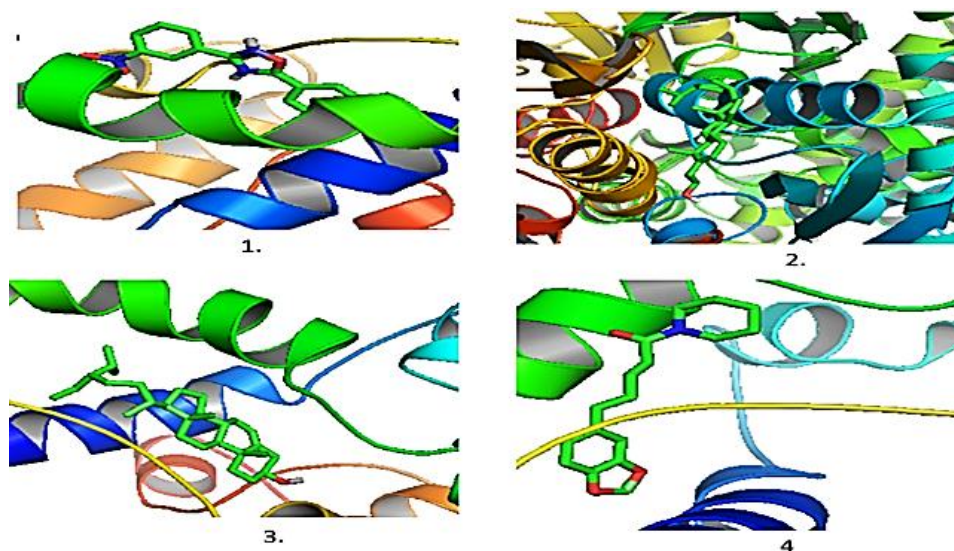


Fig 7: Ribbon representation of of protein-ligand complex (1) ERG3-Cyclohexamide (Standard) (2) ERG3- β -Sitosterol (3) ERG3- ζ -Sitosterol (4) ERG3-Piperine.

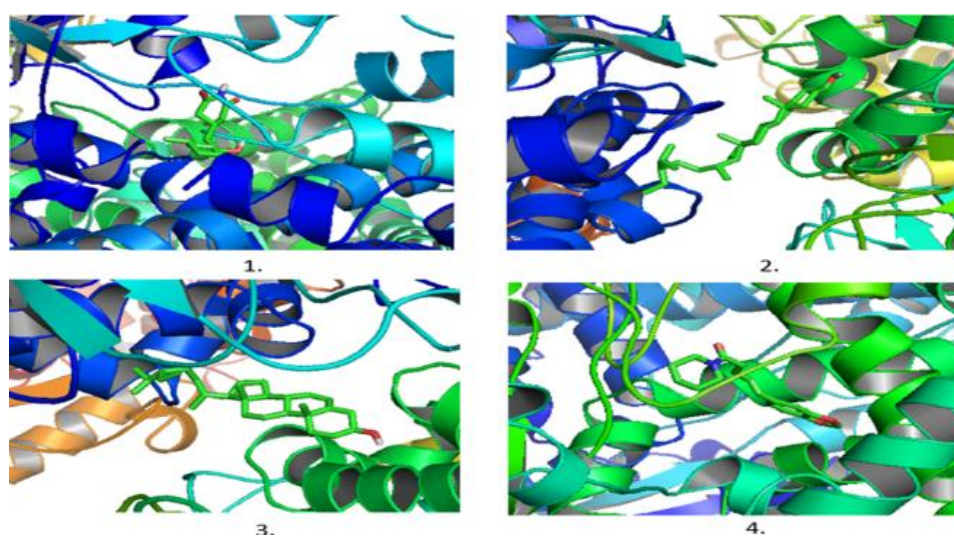


Fig 8: Ribbon representation of of protein-ligand complex (1) CaALK8-Cyclohexamide (Standard) (2) CaALK8- β -Sitosterol (3) CaALK8- ζ -Sitosterol (4) CaALK8-Piperine.

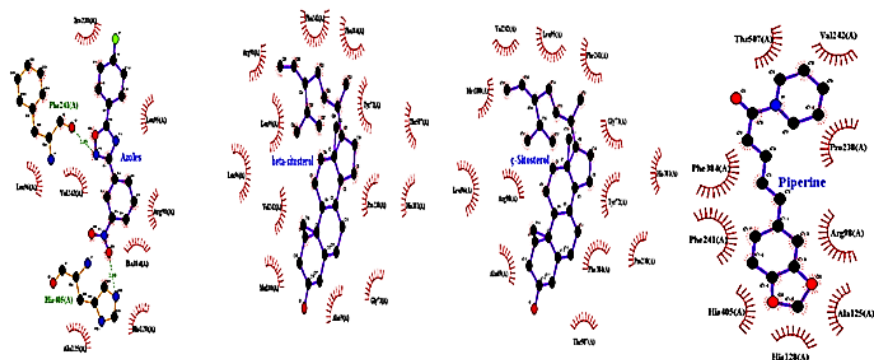


Fig 9: Azoles (Standard), β -Sitosterol, ζ -Sitosterol and Piperine binding interactions with Lanosterol 14-alpha demethylase(Erg11)

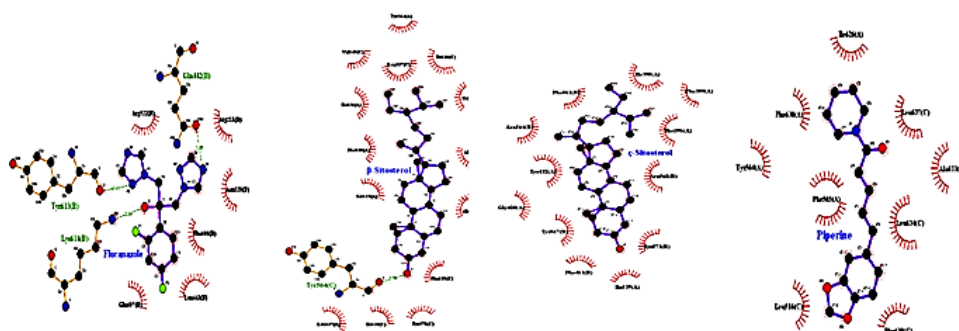


Fig 10: Flucanazole (Standard), β -Sitosterol, ζ -Sitosterol and Piperine binding interactions with CDR1

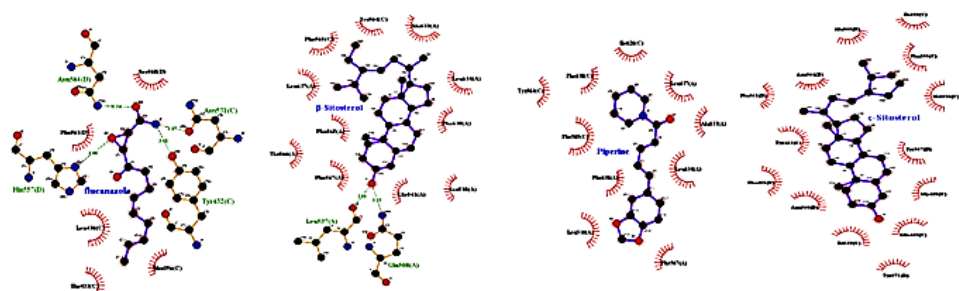


Fig 11: Flucanazole (Standard), β -Sitosterol, ζ -Sitosterol and Piperine binding interactions with CDR2.

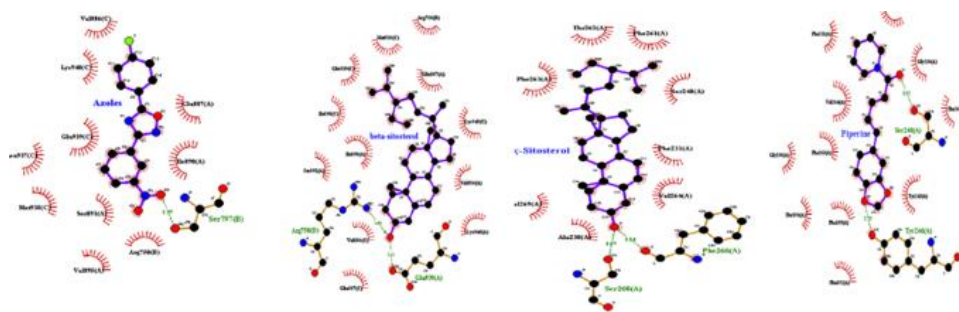


Fig 12: Azoles (Standard), β -Sitosterol, ζ -Sitosterol and Piperine binding interactions with $\Delta^5,6$ -desaturase(Erg3)

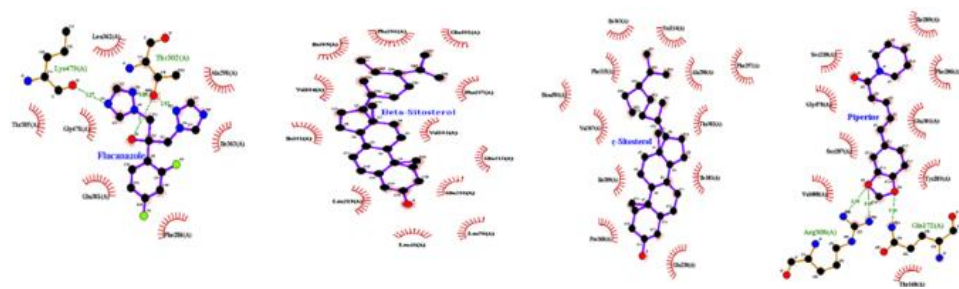


Fig 13: Flucanazole (Standard), β -Sitosterol, ζ -Sitosterol and Piperine binding interactions with C-22 sterol desaturase (Erg5)

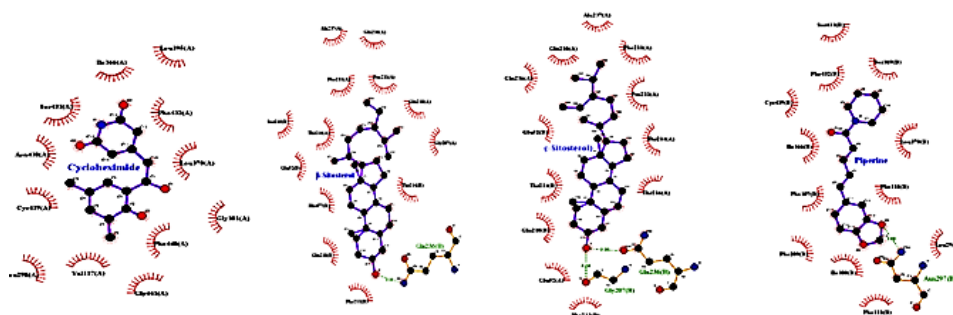


Fig 14: Cyclohexamide (Standard), β -Sitosterol, γ -Sitosterol and Piperine binding interactions with alkane assimilating cytochrome P450 (CaALK8)

Conclusion

In this study, our compounds isolated from *Parthenium hysterophorus* L. show good binding potential and follow the Lipinsky rule of five (ADME/T). So we can conclude that our selected compounds target the MDR proteins and inhibit them and maybe useful against the various fungal disease caused by the *Candida Albicans*.

Acknowledgment

The authors are thankful to the Department of Life Sciences, Mewar University, Gangrar, Chittorgarh, Rajasthan, India for providing necessary laboratory facilities. We dedicate this manuscript to Dr. Shashank Kumar, Department of Biochemistry, Central University of Punjab, Bathinda, Punjab, India for his excellent research work on in silico work on protein and ligand interactions.

Conflicting interest

The authors declare no conflict of interest.

References

- Bhat S, Mercy Lobo S, Chethan Kumar KV, Sukesh, Chandrashekar KRJ of *Phytol*. 2009; 1(6):469-474.
- Biasini M, Bienert S, Waterhouse A, Arnold K, Studer G, *et al*. SWISS-MODEL: modeling protein tertiary and quaternary structure using evolutionary information. *Nucleic Acids Res*. 2014; 42:195-201.
- Bordoli L, Kiefer F, Arnold K, Benkert P, Battey J *et al*. Protein structure homology modeling using SWISS-MODEL workspace. *Nature Protocols*. 2008; 4:1-13.
- Chothia C, Lesk AM. The relation between the divergence of sequence and structure in proteins. *EMBO J*. 1986; 5:823-826.
- Lagorce D, Sperandio H, Miteva MA *et al.*, FAF-Drugs2: free ADME\tox filtering tool to assist drug discovery and chemical biology projects, *BMC Bioinformatics* 9, 2008, 396.
- Humphrey W, Dalke A, Schulten K. VMD: visual molecular dynamics. *J Mol Graph*. 1996; 14(1):33-38.
- Jin H, Zhou Z, Wang D, Guan S, Han W. Molecular dynamics simulations of acylpeptide hydrolase bound to chlopyrifosmethyloxon and dichlorvos. *Inter J Mol Sci*. 2015; 16:6217-6234.
- Kaczanowski S, Zielenkiewicz P. Why similar protein sequences encode similar three-dimensional structures? *Theor Chem Acc*. 2010; 125:643-650.
- Nousheen L, Akkiraju PC, Enaganti S. Molecular docking mutational studies on human surfactant protein-D. *World J Pharmaceut Res*. 2014; 3:1140-1148.
- Ertl P, Rohde B, Selzer P. Fast calculation of molecular polar surface area as a sum of fragment-based contributions and its application to the prediction of drug transport properties, *J Med. Chem*. 2000; 43:3714-3717.
- Parekh J, Darshana J, Chanda S, *Turk J Biol*. 2007; 29:203-210.
- Parekh J, Darshana J, Sumitra CJ of *Biol*. 2005; 29:203-210.
- Read RJ, Adams PD, Arendall III WB, Brunger AT, Emsley P *et al*. A New generation of crystallographic validation tools for the protein data bank. *Structure*. 2011; 19:1395-1412.
- Savarino A. In Silico docking of HIV-1 integrase inhibitors reveals a novel drug type acting on an enzyme/DNA reaction intermediate. *Retrovirol*. 2007; 4:1-21.
- Schwede T, Kopp J, Guex N, Peitsch MC. SWISS-MODEL: an automated protein homology-modeling server. *Nucleic Acids Res*. 2003; 31:3381-3385.
- Trott O, Olson AJ. AutoDock Vina: improving the speed and accuracy of docking with a new scoring function, efficient optimization, and multithreading. *J Comput Chem*. 2009; 31(2):455-461.
- Georgopapadakou NH, Walsh TJ. Antifungal agents: chemotherapeutic targets and immunologic strategies, *Antimicrob. Agents Chemother*. 1996; 40:279-291.